Received: 12 January 2021 | Revised: 8 March 2021 | Accepted: 25 March 2021

DOI: 10.1096/fj.202100065R

RESEARCH ARTICLE

THE FASEB JOURNAL

Silver distribution in chronic wounds and the healing dynamics of chronic wounds treated with dressings containing silver and octenidine

Vojtěch Pavlík[1,2] | Luboš Sobotka[3] | Jaroslav Pejchal[4] | Martin Čepa[1] | Kristina Nešporová[1] | Monika Arenbergerová[2] | Adéla Mrózková[5] | Vladimír Velebný[1]

[1]Cell Physiology Research Group, Contipro a.s., Dolni Dobrouc, Czech Republic

[2]Department of Dermatovenereology, Third Faculty of Medicine, Charles University, Prague, Czech Republic

[3]Third Department of Medicine, Faculty Hospital and Medical Faculty - Charles University, Hradec Kralove, Czech Republic

[4]Department of Toxicology and Military Pharmacy, Faculty of Military Health Sciences, The University of Defense in Brno, Hradec Kralove, Czech Republic

[5]Department of Hygiene and Preventive Medicine, Medical Faculty, Charles University, Hradec Kralove, Czech Republic

Correspondence
Vojtěch Pavlík, Contipro a.s., Dolni Dobrouc 401, 56201 Dolni Dobrouc, Czech Republic.
Email: vojtech.pavlik@contipro.com

Abstract

Although silver is an efficient antimicrobial and is a widely used antiseptic in wound healing, previous studies have reported the cytotoxic in vitro effects of silver dressings. Moreover, few studies have addressed the distribution of silver in chronic wounds. The study compares the healing of chronic wounds treated with a standard-of-care silver dressing (Ag-CMC) and a dressing containing antiseptic octenidine (OCT-HA). Biopsies were taken from two wound areas before the commencement of treatment (baseline), after 2 weeks and after 6 weeks (the end of the study). We analyzed the histopathologic wound-healing score, silver distribution, and expression of selected genes. The wound-healing score improved significantly in the wounded area treated with OCT-HA after 2 weeks compared to the baseline and the Ag-CMC. The Ag-CMC wound areas improved after 6 weeks compared to the baseline. Moreover, collagen maturation and decreases in the granulocyte and macrophage counts were faster in the OCT-HA parts. Treatment with OCT-HA resulted in less wound slough. The silver, visualized via autometallography, penetrated approximately 2 mm into the wound tissue and associated around capillaries and ECM fibers, and was detected in phagocytes. The metallothionein gene expression was elevated in the Ag-CMC wound parts. This exploratory study determined the penetration of silver into human chronic wounds and changes in the distribution thereof during treatment. We observed that silver directly affects the cells in the wound and elevates the metallothionein gene expression. Octenidine and hyaluronan dressings provide a suitable alternative to silver and carboxymethyl cellulose dressings without supplying silver to the wound.

KEYWORDS

distribution of silver, hyaluronic acid, octenidine, silver, wound

Abbreviations: Ag-CMC, carboxymethyl cellulose dressing with silver; HA, hyaluronic acid; OCT-HA, wound dressing with hyaluronan and octenidine; SSD, silver sulfadiazine.

1 | INTRODUCTION

Chronic wounds are both unpleasant for the patient (pain, limited movement, social distancing, etc) and costly for the healthcare system (US$ 449-US$ 2307 per patient per year).[1] Several factors lead to the stalling of wound healing, and one of the major wound healing complications concerns bacteria.[2] Thus, antiseptics are widely used to lower the bacterial load in chronic wounds and thus to mitigate or eliminate the adverse impacts of bacteria.

Silver is an established and popular wound-healing antiseptic. The activity of the various chemical forms of silver applied (ionic silver, silver oxysalts, nanoparticles) is ensured through Ag^+ ions.[3,4] Silver ions bind to proteins and thus disrupt both their structure and function.[5] This results in the corruption of energy metabolism and the elevation of oxidative stress, which may lead to DNA damage and cellular death.[6] These effects are broad spectral and result in the elimination of gram-positive and gram-negative species. A number of studies have reported the beneficial anti-inflammatory effects of silver wound-healing products in chronic wounds.[7,8] However, other studies revealed that silver exhibits cytotoxicity toward eukaryotic cells in vitro.[9,10] Studies have even demonstrated the adverse effects of silver in the wound-healing process.[11,12]

A number of authors have detected and quantified topically-applied silver in the wounds and organs of experimental animals.[13-16] Human studies have focused on the amount of silver that penetrates from the wound dressing via the wound to the serum, liver, kidneys, and other organs.[17-19] One study analyzed the distribution of silver in a burn injury patient.[17] Recently, Roman et al analyzed the silver distribution and its chemical fate in the chronic wounds of four patients.[20]

The relatively novel octenidine antiseptic, which comprises a cationic, surface-active substance, is also used in the treatment of infected chronic wounds.[21] Octenidine disrupts bacterial cellular membranes via the destabilization of phospholipids.[22,23] Cellular death induced by octenidine occurs via a different mechanism to that of silver and is effective against multidrug-resistant bacteria (MRSA, VRE) even in their biofilm phenotypes.[24] Octenidine is considered a safe antiseptic since it does not induce skin damage in premature newborn infants or result in adverse events when applied to chronic wounds.[25,26] Moreover, octenidine evinces a lower capability with respect to penetrating through skin ex vivo.[27] A recent study has reported the similar anti-inflammatory effects of octenidine to those of silver, and the ex vivo inflammatory response of Langerhans cells to wounding was observed to diminish when treated with octenidine.[28] In addition, octenidine contributes to the healing of chronic wounds via the inhibition of the production and activity of matrix metalloproteinase and other eukaryotic proteases.[29,30] Several bacterial species produce proteases as virulence factors that contribute to the degradation of wound granulation tissue, and octenidine has even been observed to inhibit proteases secreted by bacteria that were isolated from chronic wounds.[30] In summary, octenidine positively affects the healing of chronic human wounds.[26,31]

Hyaluronan (HA) is an unbranched polysaccharide and is a natural component of skin, where it acts to maintain viscoelasticity. Apart from its structural role, hyaluronan influences the wound-healing process with respect to inflammation, epithelialization, granulation tissue formation and fibrosis.[32] HA crosslinking has the potential to enhance the number of inflammatory cells at inflammatory sites.[33] Hyaluronan cleaves (enzymatically or non-enzymatically) to smaller molecular sizes especially during inflammation. The resulting lower-molecular-weight HA evinces altered signaling properties and may act to enhance inflammation and angiogenesis.[34] Hyaluronan synthesis is initiated early in the wound-healing process, and synthesis has been observed to be sustained longer with concern to scarless fetal wound healing than to adult wound healing.[35] Further, the topical application of hyaluronan to adult human wounds improves the appearance of scars.[36,37] Keratinocytes migrate more rapidly when treated with HA in vitro; moreover, the application of hyaluronan has been observed to enhance re-epithelialization in acute animal wounds.[38] Re-epithelialization was seen to be retarded in cases where keratinocytes were unable to bind the HA (the conditional knockout of CD44—the hyaluronan receptor).[39] In short, treatment with hyaluronan significantly improves the healing of human chronic wounds, burns, and acute wounds.[40]

Despite the widespread use of silver, its distribution in chronic human wounds and wound healing has not been adequately described to date. Thus, the study aimed to compare the healing of chronic human wounds via the application of wound dressings containing silver and dressings containing octenidine. We treated different parts of the same large wounds simultaneously with the two dressings, an approach that allowed us to directly compare the effects of the dressings on wound healing and to evaluate the distribution of silver over time.

2 | MATERIALS AND METHODS

2.1 | Ethics

The study was conducted in compliance with the current version of the Declaration of Helsinki. The Ethical Committee of the Faculty Hospital in Hradec Kralove, Czech Republic, approved the study protocol and the experimental protocol (201405 S10ZP). The experiments were performed in

accordance with the relevant guidelines and regulations. All the patients in the study provided their written informed consent.

2.2 | Patient inclusion and exclusion criteria

The study participants were selected according to the following inclusion criteria: age 60-90 years; non-healing leg wound for ≥6 weeks; wound size of 100-400 cm^2; willingness to participate in the study.

The exclusion criteria were as follows: autoimmune disorders; ongoing oncological treatment; treatment with antibiotics (systemic or local) ≤ 1 week before the start of the trial; pregnancy or lactation; sensitivity to the active compounds of the proposed dressings; known alcohol or substance abuse; renal insufficiency or liver failure; deep venous thrombosis or varicose vein surgery less than three months before the baseline of the trial; participation in another trial that may have interfered with the results.

2.3 | Patient characteristics

Nine patients entered the study, which was scheduled to run for 6 weeks. Seven patients finished the 6-week treatment. One patient healed before the end of the 6-week evaluation period, and one patient did not finish the study due to reasons not connected with the trial. Three patients had diabetes mellitus type II. Five patients were women (72.2 ± 7.6 y), four were men (74.5 ± 11.2 y). The ulcers were caused by venous (n = 5), or mixed with dominant venous (n = 4) insufficiency. The patients were hospitalized at the Third Department of Medicine, Faculty Hospital and Medical Faculty, Charles University in Hradec Kralove, Czech Republic.

2.4 | Study protocol

Following debridement, the wound of each patient was divided into two parts and randomized for treatment. The wounds were treated with OCT-HA (Sorelex, Contipro a.s, Dolni Dobrouc, Czech Republic) and Ag-CMC (Aquacel Ag+, Convatec, Berkshire, UK) dressings. Both the OCT-HA and Ag-CMC dressings were covered with several layers of sterile gauze, that is, a secondary dressing which was changed daily. It was verified that the dressings were unable to move beneath the secondary dressings and, thus, potentially influence the wound-healing process outside of the intended area. The minimal displacement of the dressings was also supported by the fact that the patients were hospitalized during the whole of the study. The percentage of the wounds covered by slough was assessed at weeks 0, 2, 4, and 6. Biopsies were taken using a bioptic punch (4 mm, Kai Medical, Seki, Japan) following local anesthesia (1.8 mL Marcaine 5 minutes prior to the procedure) at weeks 0, 2, and 6. The biopsies were taken as far away as possible from the part of the wound treated with the second dressing so as to minimize the mutual influence of the investigated changes. The silver autometallography of the OCT-HA samples confirmed that the Ag-CMC dressings had not leaked silver into the OCT-HA-treated parts of the wounds. Moreover, the biopsies were taken a minimum of three centimeters away from previous biopsy areas so as to minimize the effect of the close harvesting of the tissue. The taking of the wound biopsies did not negatively affect the overall wound-healing process.[41] Nevertheless, the biopsy sites were monitored for possible wound-healing complications.

2.5 | Processing of the histological samples

Formaldehyde-fixed tissue samples were dehydrated via the use of increasing concentrations of ethanol and xylene (Penta, Prague, Czech Republic) and transferred to liquid paraffin using a Leica TP1020 processor (Leica, Wetzlar, Germany). Subsequently, the samples were embedded in the paraffin and cooled using an EG1150H (Leica) paraffin embedding station, and 5 μm sections were cut using an RM 2250 (Leica) rotary microtome. The sections were hydrated using xylene, decreasing concentrations of ethanol and deionized water (Aqual 29; Aqual, Brno, Czech Republic), followed by staining.

The hydrated samples were stained with hematoxylin and eosin (both from Merck, Kenilworth, NJ, USA) according to the manufacturer's instructions, dehydrated and mounted into a Pertex (Histolab, Västra Frölunda, Sweden) aqueous-free mounting medium.

With respect to the Masson's trichrome staining, hydrated samples were stained with Weigert's hematoxylin (50 minutes; Bamed, Ceske Budejovice, Czech Republic) and differentiated. The differentiated samples were then immersed in Ponceau solution (1% of xylidine Ponceau, 1% of phosphotungstic acid [both from Bamed], and 1% of glacial acetic acid [Sigma-Aldrich, St. Louis, USA]) with acid fuchsin (1% of acid fuchsin [Bamed] and 1% of glacial acetic acid) for 5 minutes, rinsed with deionized water, and stained with 1% of phosphotungstic acid (5 minutes). The samples were immersed in an aniline blue solution (comprising 2.5% of aniline blue [Bamed] and 2.5% of glacial acetic acid). The subsequent differentiation was conducted using 1% of acetic acid. The samples were mounted into an ImmunoHistoMount (Sigma-Aldrich) aqueous-based mounting medium.

Hydrated samples were stained using the Van Gieson's picrofuchsin kit (Cat. No. C0602; DiaPath, Martinengo, Italy) according to the manufacturer's instructions. The samples

were then dehydrated and mounted into a DPX aqueous-free mounting medium (Sigma-Aldrich).

Hydrated samples were stained using a naphthol AS-D chloroacetate esterase kit (Cat. No. 91C-1KT; Sigma-Aldrich) according to the manufacturer's instructions. The samples were mounted into an ImmunoHistoMount aqueous-based mounting medium (Sigma-Aldrich).

The silver autometallography was performed according to Danscher et al[42] Hydrated samples were immersed in 0.5% of gelatin (Sigma-Aldrich) and dried at 20°C for 20 minutes. The slides were then coated with a developing agent (30% of Gum arabic, 2.55% of citric acid, 2.35% of sodium citrate, 0.85% of hydroquinone, and 0.11% of silver lactate [all from Sigma-Aldrich]) in darkness at 20°C for 90 minutes. The samples were rinsed with warm tap water for 20 minutes and immersed in 0.9% of sodium thiosulfate (Sigma-Aldrich) and 0.1% of sodium ferrocyanide (Merck) for 19 seconds, rinsed with deionized water, dehydrated, and mounted into Pertex.

2.6 | Histological evaluation

The following parameters were evaluated using an Olympus BX51 microscope (Olympus, Tokyo, Japan) by a histopathologist who was blinded to the treatment.

The histopathological score was defined via the sum of six parameters (Table S1) according to Sultana et al[43] Parameters 1-4 were evaluated for the hematoxylin-eosin stained samples and parameters 5 and 6 were evaluated for the Masson's trichrome stained samples. The healing status was classified according to the histopathological score as poor (6-11), fair (12-15), and good (16-20).

The wound slough was assessed for the hematoxylin-eosin stained samples according to the semiquantitative score as high—1, moderate—2, minimal—3, focal—4, absent—5. Grades 1—3 represented a wound slough layer that extended over the whole of the wound bed of the biopsy.

The average count of naphthol AS-D chloroacetate esterase-positive cells per microscopic field was obtained using an Olympus DP73 camera and ImagePro 5.1 computer image analysis software. The cells were tagged manually and counted in six randomly selected microscopic fields per sample at 400× magnification. The microphotographs were taken from the area of newly formed connective tissue in close vicinity to the wound bed.

The percentage content of collagen fibers per microscopic field (Van Gieson's picrofuchsin) was evaluated using a camera with computer image analysis. The positivity was detected within the Red/Green/Blue scale in the ranges: red 180-218, green 62-128, and blue 121-185, and expressed in percent (%). Six microscopic fields were randomly selected from the area of newly formed connective tissue in close vicinity to the wound bed.

The distribution of silver ions was evaluated over the whole extent of the wound biopsy in the silver-stained samples.

The statistical significance of the differences in the evaluated histological parameters was assessed using the Wilcoxon rank-sum paired test (IBM SPSS Statistics 24, IBM Corporation, Armonk, NY, USA). The test was applied for the statistical analysis of the Ag-CMC and OCT-HA samples at particular times. The differences were considered significant if $P \leq .05$.

2.7 | Fluorescence microscopy

Histological sections on Superfrost PlusTM glass slides (Thermo Fisher Scientific, Waltham, MA, USA) were deparaffinized and incubated overnight with a primary antibody (1:100, CD68 Antibody (KP1), MA5-13324, Thermo Fisher Scientific), followed by 90 minutes of incubation with a secondary antibody with Alexa Fluor 555 (ab150114, Abcam, Cambridge, UK; dilution 1:10 000) and mounting with ProLong Diamond Antifade Mountant with DAPI (ThermoFisher Scientific). The sections were imaged using a Leica TCS SP8 X confocal microscope with a Leica HC PL APO CS2 objective (20×, 0.75 NA, water) and a 405 nm laser line for the DAPI excitation and a 550 nm white light laser line for the Alexa 555 excitation. The images were acquired in z-stacks covering the thickness of the whole of the section applying 1.8 μm steps in the quantitative mode. A maximum intensity projection was performed in the fluorescence channels. The fluorescence quantification of all the images was performed using FiJi software.[44] The fluorescence intensity was analyzed in three to five fields near the wound bed. The results were expressed as an average percentage of the pixels above the threshold (30 for all the images). The cutoff value for the threshold was determined using a negative control image (secondary antibody only). The statistical significance of the differences between the samples was evaluated via the Wilcoxon rank-sum paired test in R.[45] The test was used for the statistical analysis of the Ag-CMC and OCT-HA samples at particular times.

2.8 | Gene expression analysis

The RNA isolation, cDNA synthesis, and qPCR gene expression analysis were performed as previously described.[46] The TaqMan Real-Time PCR Assays (ThermoFisher Scientific) used for the qPCR analysis comprised: IL1B—Hs01555410_m1; TNF—Hs01113634_g1; CD3E—Hs01062241_m1, CD4—Hs01058407_m1; CD8A—Hs00233520_m1; CD14—Hs02621496_s1; MT1G—Hs01584215_g1; MT1H—Hs00823168_g1; GADD45G—Hs00198672_m1; RPL13A—Hs04194366_g1. The threshold cycle values were

normalized to the RPL13A housekeeping gene and related to the average of the biopsies sampled prior to the treatment of the respective patient via the $2^{-\Delta\Delta Ct}$ method.[47] The significance of the differences in the gene expression at each time point was evaluated using the paired Wilcoxon signed-rank test in R.

3 | RESULTS

Patients with large chronic wounds were treated with a standard-of-care dressing containing silver-impregnated carboxymethyl cellulose (Ag-CMC, Aquacel Ag+ Extra) and a dressing containing octenidine with hyaluronan on a polyester secondary layer (OCT-HA, Sorelex). Biopsies were taken from the wounds before treatment and after 2 and 6 weeks of treatment. The distribution of silver in the biopsies was visualized by means of silver autometallography (Figure 1). Although no silver staining was apparent prior to treatment (Figure 1A), silver was detected relatively deep (more than 2 mm) within the granulation tissue after 2 and 6 weeks of treatment (Figure 1B,C). The distribution of the silver was heterogeneous. As neovascularization progressed, silver positivity dominated around the adventitial and periadventitial tissue (Figure 1D). As the granulation tissue matured, positive silver staining became increasingly apparent around the ECM filamentous structures, and the positivity around the vasculature was observed to be less pronounced than in the earlier wound stages (Figure 1E,F).

Silver was also detected in phagocytes (Figure 2A) in the area rich in CD68+ macrophages (Figure 2B,C). Unfortunately, the phagocytes could not be concomitantly stained for silver and CD68 since the staining protocols were not compatible. The amount of CD68 signal present near the wound bed was evaluated using IHF. The amount of the CD68 signal increased in 5 out of 7 samples after 2 weeks of treatment with Ag-CMC and in 4 out of 7 samples after 6 weeks of treatment. The increase was not statistically significant for either the 2- or 6-week interval when compared to the baseline.

In contrast, the CD68 signal was significantly lower in those parts of the wounds treated with OCT-HA than those treated with Ag-CMC (Figure 3). Moreover, the parts of the wounds treated with Ag-CMC exhibited significantly higher numbers of granulocytes (marked by the esterase activity toward naphthol AS-D chloroacetate), (Figure 3). A significant

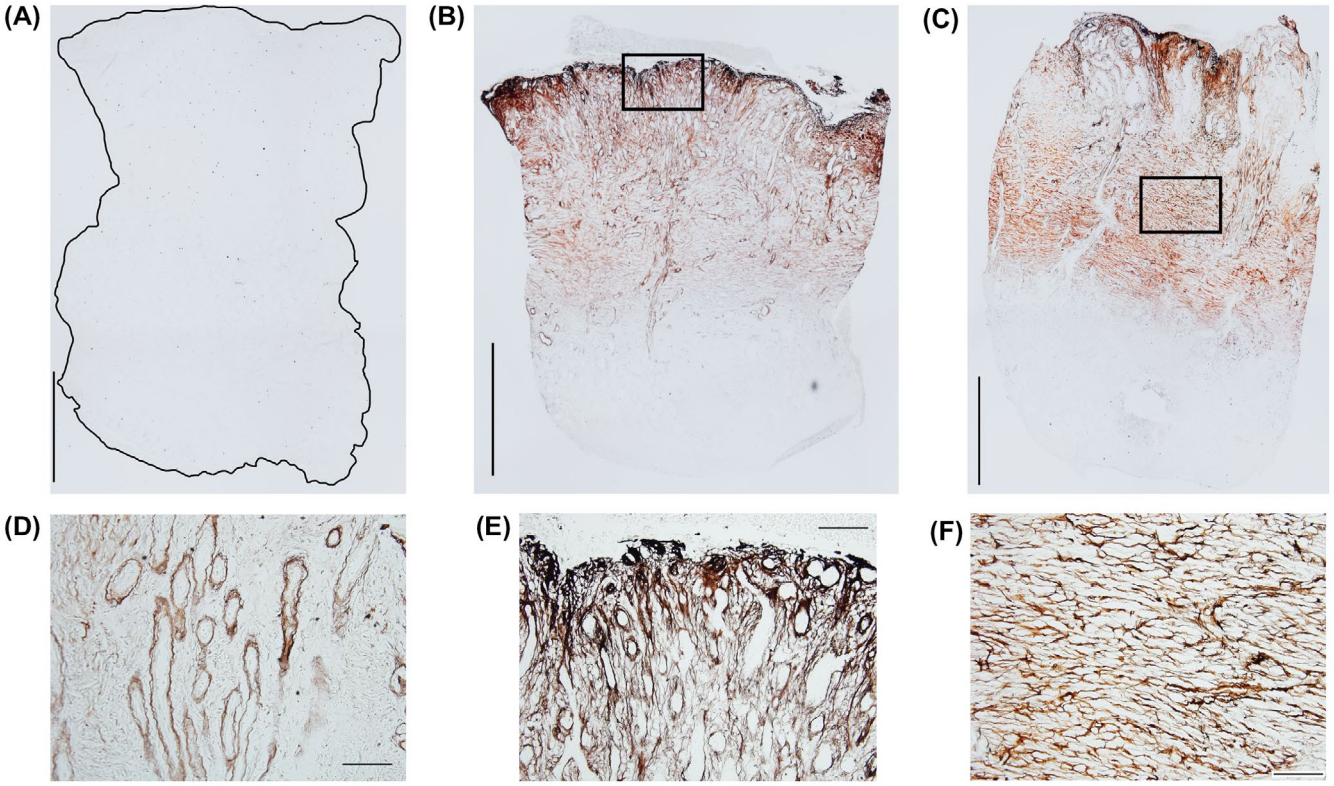

FIGURE 1 Silver distribution patterns in chronic wounds. Wound biopsies from the Ag-CMC part of the wound (female, 83). The top-row images are oriented with the wound bed facing upwards. A, A sample prior to treatment with the silver dressing (the outline of the sample was traced post-acquisition so to highlight its boundaries), (B) after 2 weeks of treatment, (C) and 6 weeks of treatment with Ag-CMC. The scale bars (A-C) correspond to 1 mm. D, Staining was apparent around the veins in the periadventitial space (male, 68). E, As wound healing progressed, the positivity of the veins was less apparent and, subsequently (F) the association of silver with the fibrillar ECM dominated. Images (E) and (F) are magnifications of (B) and (C), respectively, from the areas indicated by the rectangles. The scale bars (D-F) correspond to 50 μm

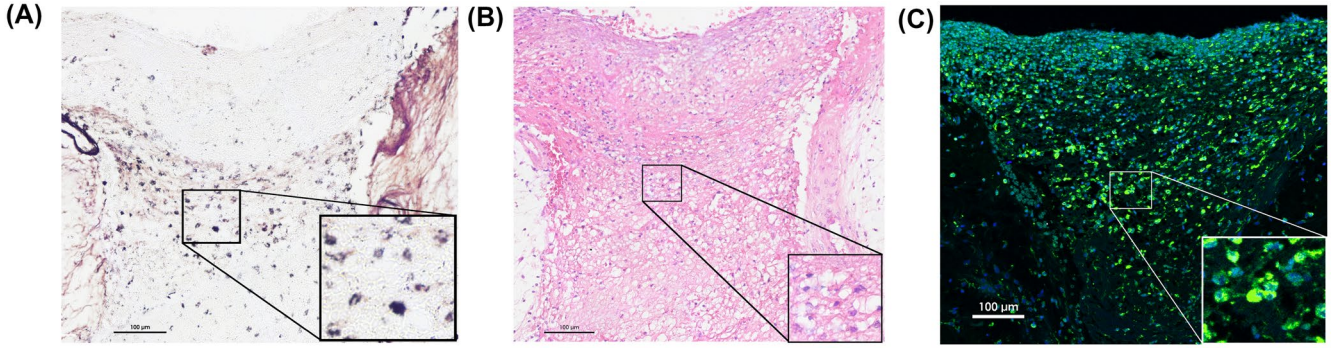

FIGURE 2 Silver in phagocytes. Phagocytes containing silver visualized via silver autometallography (A), the corresponding area stained with HE (B) and with the antiCD68 antibody with DAPI nuclear counterstaining (C), (female, 74). The scale bars correspond to 100 µm

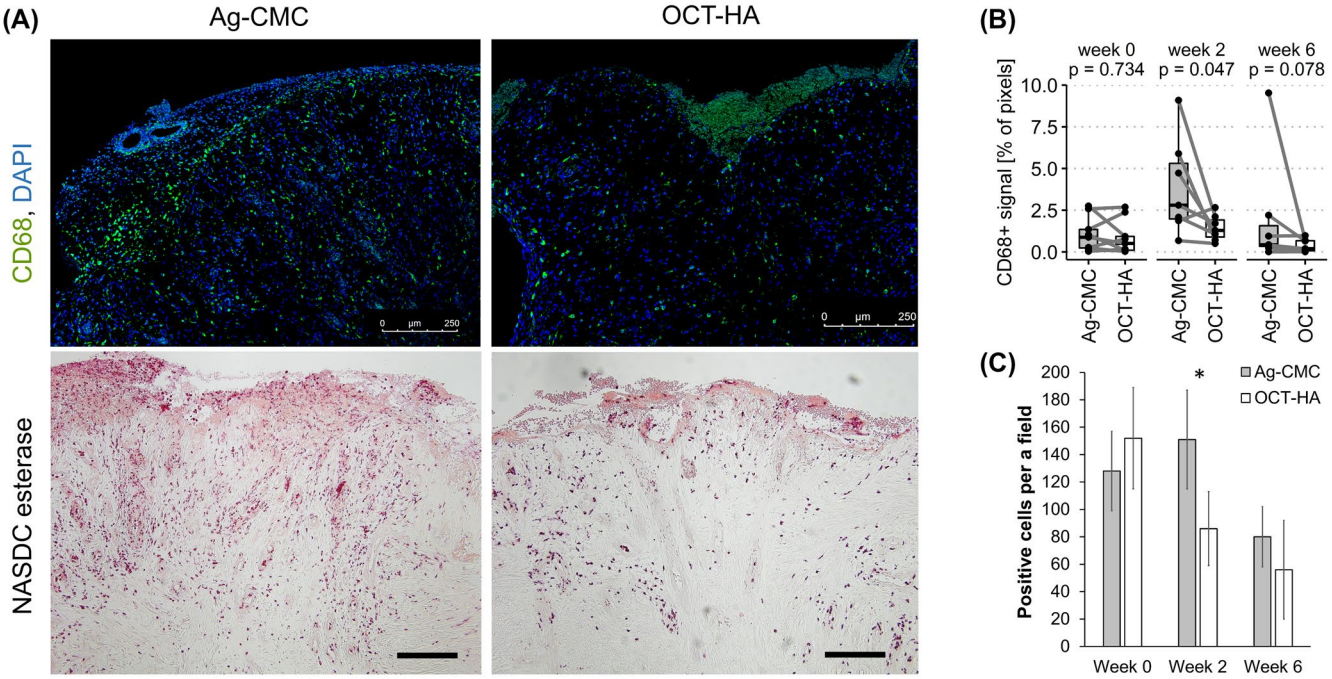

FIGURE 3 Granulocytes and macrophages in the wound biopsies. A, A set of representative images stained with the antiCD68 (macrophages) antibody in biopsies from the Ag-CMC-treated and OCT-HA-treated parts of the wound of the same patient (female, 74). The lower set of images shows the histochemical staining of the naphthol AS-D chloroacetate esterase activity (granulocytic lineage cells) in biopsies treated for 2 weeks with Ag-CMC and OCT-HA (male, 68). B, The evaluation of the CD68 signal in the corresponding parts of the wounds treated with Ag-CMC and OCT-HA. The boxplots illustrate the median and interquartile ranges. The gray lines connect the biopsies from the same wound at a given time. Wilcoxon rank-sum test (n = 9 for weeks 0 and 2, n = 7 for week 6). C, The quantification of naphthol AS-D chloroacetate synthesis positive cells via image analysis. The values represent the mean ± SD from six non-overlapping microscopic fields per sample at 400× magnification. $^*P \leq .05$ Wilcoxon paired rank-sum test. The scale bars correspond to 250 µm

decrease in granulocytes from the baseline values occurred after 2 weeks of OCT-HA treatment and after 6 weeks of Ag-CMC treatment. A portion of each wound biopsy was analyzed for gene expression changes in inflammatory cell markers (Figure 4A). *CD14*, which is widely expressed by monocytes and macrophages, was observed to be upregulated in the Ag-CMC parts of the wounds after 2 and 6 weeks of treatment. The gene expression of the *CD4* T-cell marker was significantly lower in the OCT-HA parts of the wounds after 2 weeks, and decreased more rapidly than in the Ag-CMC parts. The gene expression of *CD8A* was enhanced (although not statistically significantly) in the Ag-CMC parts, and *CD3E* was expressed in both the CD4+ and CD8+ T cells. We also measured a lower, although statistically insignificant, *CD3E* expression in the OCT-HA-treated wound parts. In order to reflect the presence of classic pro-inflammatory cytokines, we also measured the gene expression levels of *IL1B* and *TNF* (Figure 4B).

Although both of the pro-inflammatory mediators decreased as the wounds healed, the decrease was more

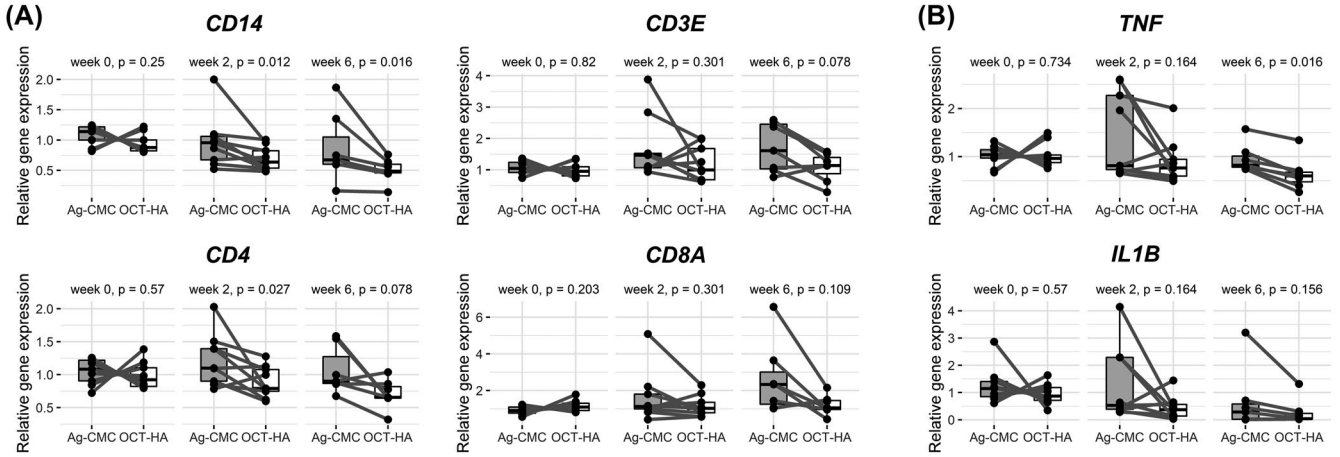

FIGURE 4 The gene expression analysis of inflammatory cell markers and mediators. A, The gene expression of the *CD14* monocyte/macrophage marker gene and the *CD3E, CD4,* and *CD8A* T-lymphocyte markers. B, The gene expression of pro-inflammatory markers in biopsies taken at weeks 0, 2, and 6 from parts of a wound treated with Ag-CMC and OCT-HA. The boxplots illustrate the median and interquartile ranges. The gray lines connect the gene expression values from the same wound and time. The *P* values above the boxplot pairs highlight the significance of the differences between the two approaches at corresponding times and were calculated via the Wilcoxon rank-sum test (n = 9 for weeks 0 and 2, n = 7 for week 6)

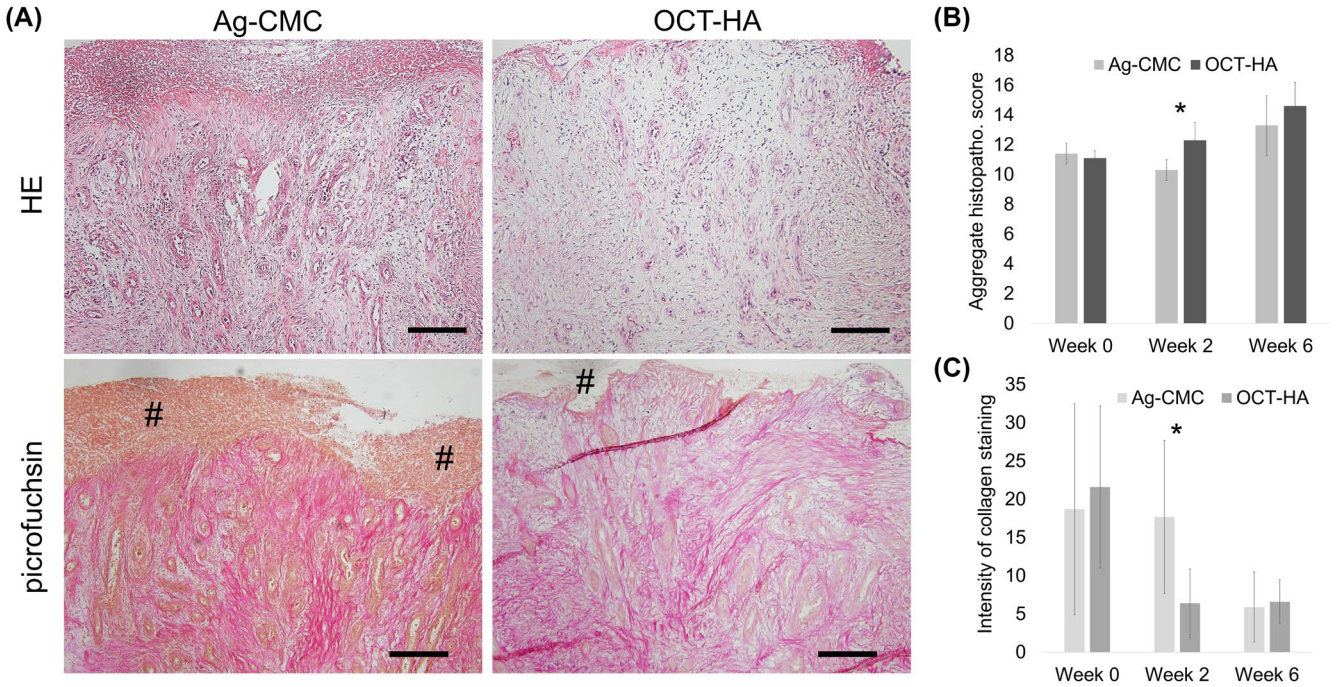

FIGURE 5 Wound-healing histopathology. A, A representative histological evaluation of the part of a wound (male, 68) treated for 2 weeks with Ag-CMC (the left set of images) following HE staining and picrofuchsin staining. Moderate amounts of granulation tissue and inflammatory infiltrate are present under a thick layer of wound slough (#). The collagen (pink) orientation is mainly vertical and the collagen pattern is mixed. The aggregate histopathological score of the Ag-CMC part of the wound according to Sultana et al[43] was 10. The right set of images show a biopsy from the same wound as described above from the part of the wound treated with OCT-HA. The layer of wound slough is thin (#) and is accompanied by only scanty granulation tissue and a moderate amount of inflammatory infiltrate. The collagen orientation and pattern are mixed. The aggregate histopathological score of the OCT-HA part of the wound was 12. B, The total score of the histological parameters. A higher score signifies more advanced healing. $*P \leq .05$, n = 7, Wilcoxon paired rank-sum test. C, Computational image analysis of the collagen intensity staining of samples stained by means of the Van Gieson's picrofuchsin method. The collagen staining decreases as the wound heals. Image of the sample from the OCT-HA part stained by means of picrofuchsin features four dark pink lines (interfolds) which comprise artifacts from the preparation of the sample. Mean ± SD. $*P \leq .05$, n = 7, Wilcoxon paired rank-sum test. The scale bars correspond to 500 μm

pronounced with concern to the OCT-HA-treated parts of the wounds (statistically significant for TNF after 6 weeks).

In addition to inflammation, we also investigated several histological parameters of wound healing status in the Ag-CMC- and OCT-HA-treated parts of the wounds according to Sultana et al[43] The assessed parameters (amount of early or late collagen, the orientation of collagen fibers, the amount of granulation tissue, the presence of immune cells in HE-stained sections) were scored according to a semiquantitative scale, then summed and expressed as a wound healing score, based on which the wounds were seen to have healed significantly faster in the OCT-HA-treated parts after 2 weeks of treatment (Figure 5, Table S2).

The histological score improved in the Ag-CMC-treated parts of the wounds only later, as evinced by the analysis after 6 weeks of treatment.

We subsequently investigated the percentage of collagen near the wound bed in the histological sections by means of image analysis (Figure 5). The intensity of the collagen staining decreased as the granulation tissue matured. After 2 weeks of treatment with OCT-HA, a significant improvement was observed in terms of this parameter. A significant decrease in collagen staining was observed in the Ag-CMC parts of the wounds after 6 weeks of treatment.

As wounds heal, the wound slough should diminish. The wound beds treated with Ag-CMC for 2 weeks contained significantly more slough than the corresponding OCT-HA-treated parts, which was evident from the samples stained with picrofuchsin (Figures 5A and 6A). The macroscopic observation concurred with these results, and confirmed that wound slough covered a higher proportion of the wounds treated with Ag-CMC than those treated with OCT-HA after 2, 4, and 2 weeks (Figure 6B,C).

Silver (and certain other metals) induces an increase in the gene expression of metallothioneins in cells, which serves to mitigate the toxicity of the metal. Hence, we assayed the gene expression of *MT1G* and *MT1H*, which was observed to be markedly elevated and attained statistical significance with respect to *MT1H* after 2 weeks of treatment with the silver dressing compared to the parts of the wounds treated with OCT-HA (Figure 7).

4 | DISCUSSION

Silver was detected via silver autometallography in the granulation tissue of the chronic wounds to a depth of approximately 2 mm. A study by Rigo et al detected silver from a dressing

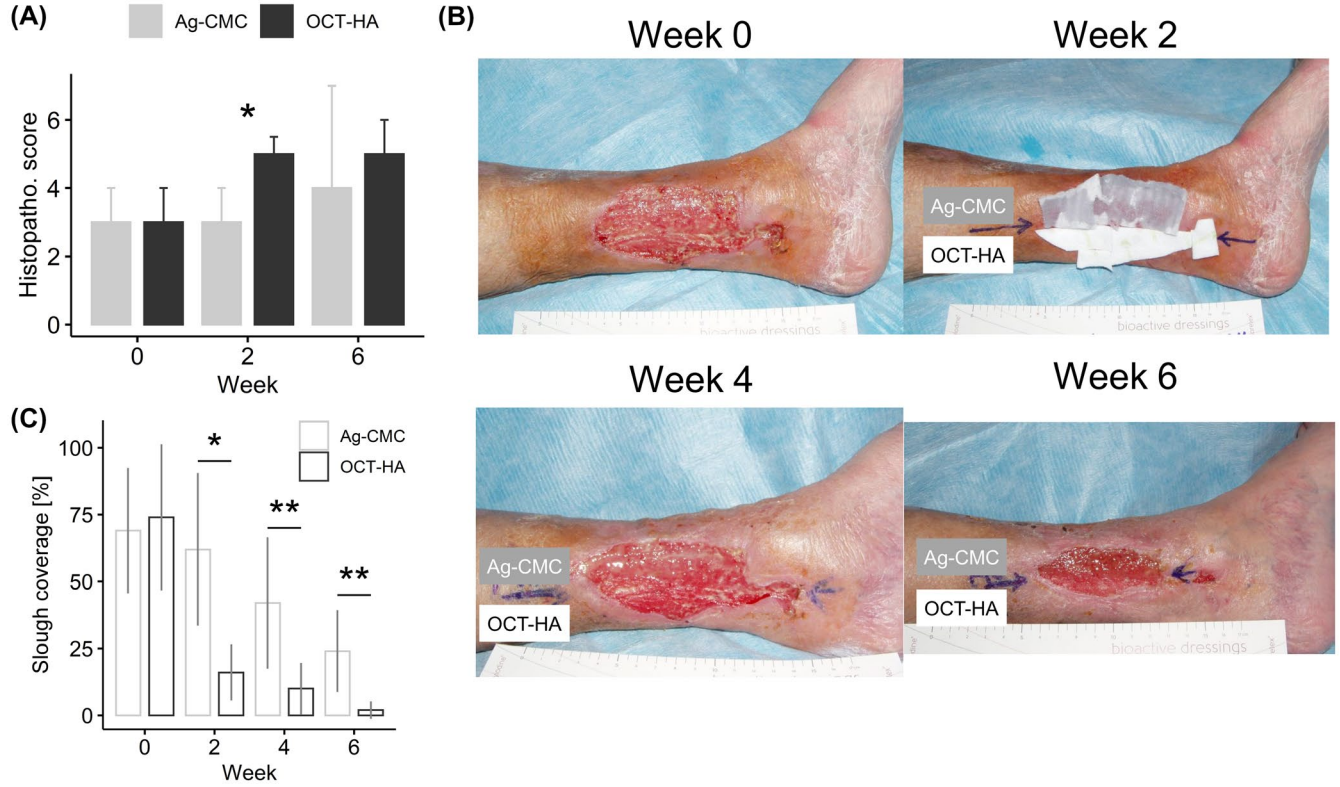

FIGURE 6 Wound slough. A, The wound slough was evaluated in IHC sections according to a semiquantitative scale (high 1—absent 5) and expressed as the median ± IQR. *$P \leq .05$ Wilcoxon paired rank-sum test. B, Macroscopic overview of the wound-healing process for the Ag-CMC and OCT-HA, and the quantification of the wound slough (female, 83). Half of the wound was treated with Ag-CMC and half with OCT-HA. The appearance of the wound prior to treatment, with the applied dressings, after 2 weeks and after 6 weeks of treatment. C, Macroscopic assessment of the wound bed slough coverage. Mean ± SD. *$P \leq .05$, n = 7, Wilcoxon paired rank-sum test

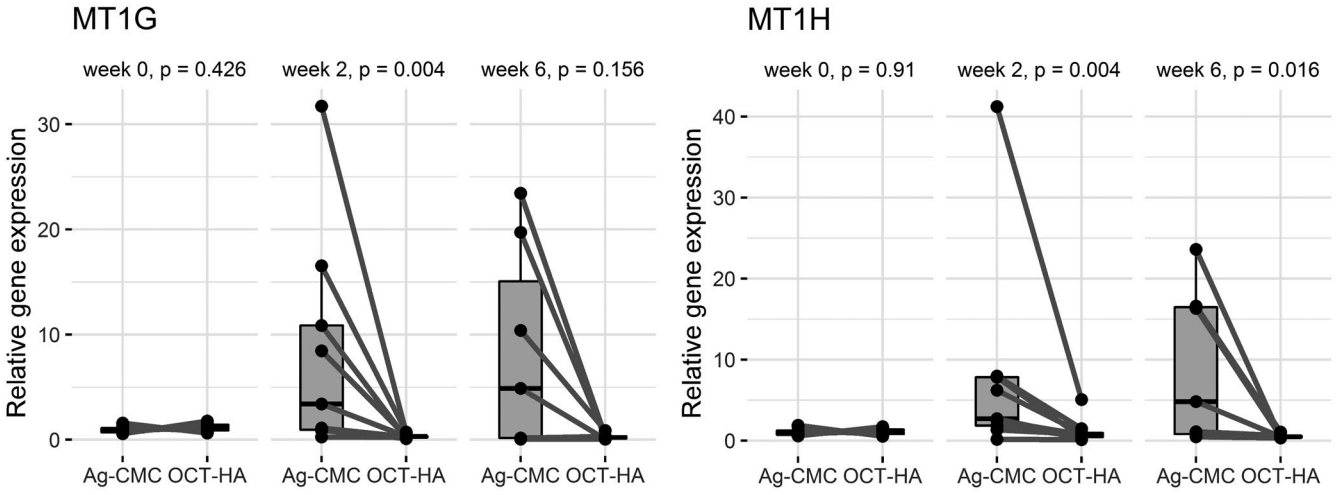

FIGURE 7 The gene expression of *MT1G* and *MT1H* metallothioneins in biopsies taken at weeks 0, 2, and 6 from the parts of the wounds treated with Ag-CMC and OCT-HA. The boxplots illustrate the median and interquartile range. The gray lines connect the gene expression values from the same wound and time. The *P*-values illustrate the significance of the differences between the two treatment approaches at corresponding times. Wilcoxon paired rank-sum test (n = 9 for weeks 0 and 2, n = 7 for week 6)

Acticoat Flex 3 with nanoparticles at a depth of 4 mm in a burn wound using TEM, that is, twice the depth indicated by our results.[17] We applied a dressing containing silver chloride, which may well penetrate at a different rate to that of silver nanoparticles, with respect to which the shape of the nanoparticles may also influence the degree of penetration through skin. Rods have been observed to be more effective in terms of penetration through mouse skin into the blood than spheres or triangles.[48] Roman et al detected the majority of silver nanoparticles in chronic wounds up to a depth of 1.5 mm.[20]

We observed the association of silver with elastic and collagen fibers and localization around capillaries in the chronic wounds. Fredriksson et al observed a similar silver distribution pattern in ex vivo explanted human skin treated with the same silver dressing (Aquacel) as used in this study.[49] Similar silver distribution patterns were also observed in several studies that investigated argyria in the eye following the application of eye-drops containing silver, and skin argyria as a result of acupuncture using silver needles.[19] Admittedly, argyria, which creates insoluble silver deposits, is a somewhat extreme case (although observed in wound healing[50]) of long-term exposure to silver.

The enhanced presence of silver around capillaries observed in this and the aforementioned studies suggests a passive silver elimination pathway from wounds to the blood. It has been demonstrated previously that silver associates with serum proteins such as albumin, as well as with glutathione.[51] Enhanced levels of serum albumin in patients with chronic wounds serve for protection against increased silver concentrations in the blood.[52] The speciation of silver presented in a study by Roman et al suggested that silver binds predominantly to chloride in the upper layers (up 45 μm) and to glutathione in the deeper parts of the wound.[20] Therefore, silver-protein complexes may well provide a silver removal pathway from wounds.

A further approach to eliminating silver from wounds comprises phagocytosis. We discovered cells (probably macrophages) loaded with silver in the wound biopsies. Macrophages are capable of the engulfment of silver nanoparticles.[53] In vitro studies have revealed that the phagocytosis of silver nanoparticles both enhanced inflammation and damaged macrophages.[54,55] It is, therefore, possible that macrophages in chronic human wounds are also damaged by phagocytosed silver. Consequently, silver-treated wounds would require a greater amount of macrophages in order to remove debris and to participate in other wound-healing processes. Our results revealed significantly higher numbers of macrophages in the Ag-CMC-treated parts of the wounds than in the OCT-HA-treated parts. Souza et al demonstrated an increase in the number of macrophages during the granulation phase of the healing of a burn wound in a rat following treatment with SSD (silver sulfadiazine).[56]

In tandem with the presence of silver as revealed via autometallography, we further discovered that the silver released from the silver dressing acted to elevate the expression of metallothionein genes. It has been determined that the gene expression of metallothioneins increased following the stimulation of macrophages with Ag^+ in vitro[57] and in vivo in the lungs when exposed to silver nanoparticles.[58] Moreover, Lansdown et al observed the elevated production of metallothionein in sterile rat wounds treated with silver sulfadiazine.[59] In addition to metals, cellular stress also induces the expression of metallothioneins, which play anti-inflammatory and cytoprotective roles.[60] The gene expression of metallothioneins was detected in our samples at week 0 (prior to treatment with Ag-CMC and OCT-HA), which most likely corresponded to the natural

cytoprotective role it plays in (chronic) wounds. Subsequently, however, the Ag-CMC treatment acted to elevate the metallothionein gene expression, most likely in order to mitigate the silver oxidative effects.

We compared Ag-CMC and OCT-HA wound dressings side-by-side in chronic human wounds. Although both parts of the wounds healed, we detected differences in both the inflammation resolution and the ECM maturation in favor of OCT-HA. Moreover, the appearance of the wound bed and the slough coverage were seen to be better following OCT-HA treatment. A decrease in the numbers of neutrophils and macrophages, which is necessary in order to mitigate the inflammatory phase, was observed in the parts of the wounds treated with OCT-HA within 2 weeks of treatment, whereas a decrease in the presence of neutrophils and macrophages was observed later (between weeks 2 and 6) with respect to the Ag-CMC dressings. Correspondingly, the gene expression of the *TNF, IL1B,* and *CD4* pro-inflammatory markers decreased more prominently in those parts of the wounds treated with OCT-HA. In line with our results, Krasowski et al demonstrated via a randomized controlled trial that treatment with octenidine supported wound healing to a greater extent than did a silver dressing.[61]

We noticed the differences between the two approaches primarily after 2 weeks of treatment. After 6 weeks of treatment, no significant difference was apparent between the Ag-CMC and OCT-HA approaches in terms of the collagen intensity staining or the number of neutrophils. With regard to the collagen intensity staining, the minimum of this parameter (the lower the better) was attained in the OCT-HA parts after 2 weeks and remained the same for a further 4 weeks, suggesting that no further decrease was likely in terms of this parameter during the wound-healing process. The Ag-CMC parts of the wounds attained the collagen staining minimum significantly later.

A decrease was observed in the number of neutrophils in the OCT-HA parts of the wounds after 2 weeks, and the decrease continued until the sixth week of treatment. The Ag-CMC parts evinced an increase in neutrophils after 2 weeks of treatment followed by a decrease to similar values as observed in the OCT-HA parts. The possibility cannot be excluded in this respect that the earlier resolution of inflammation in one part of the wound may have expedited the resolution of inflammation in the other part. Thus, the healing of both parts would converge due to paracrine signaling from the cells in the better healed part of the wound. Previously, granulation tissue has been transplanted within a wound so as to expedite healing in problematic areas (eg, on exposed bone).[62] Chen et al isolated cells from the healing granulation tissue of control mice and injected them into a wound margin of γ-irradiated mice.[63]

Our results did not indicate that silver evinces an anti-inflammatory effect in chronic human wounds. Indeed, other studies have even shown that silver acts in a pro-inflammatory manner in model animals. Silver sulfadiazine (SSD) was observed to retard the healing of a burn wound in mice and to induce an increase in the number of neutrophils and a decrease in the amount of macrophages.[12] Similarly, nanocrystalline silver (Acticoat) was seen to more than double the number of pro-inflammatory cells in acute porcine wounds, although the overall wound healing rate was not affected.[64]

In contrast, Nadworny et al applied solutions of a nanocrystalline dressing to dermatitis (dinitrochlorobenzene-induced inflammation in pigs) and subsequently observed decreased inflammation.[65] Thomason et al reported a decrease in inflammation in mice wounds following the application of silver oxysalts.[66] Lansdown et al presented mitigated inflammation in rat wounds following treatment with SSD.[59] Silver nanoparticles embedded in a collagen/chitosan gel promoted wound healing and decreased the number of CD68+ cells and the levels of pro-inflammatory cytokines in rat skin wounds.[67] Silver sulfadiazine (SSD) was observed to decrease the neutrophil and macrophage count in chronic human wounds relative to the control as the wounds were healing; however, PVP-I and chlorhexidine digluconate were seen to decrease the presence of pro-inflammatory cells even more rapidly than did SSD.[11] However, none of these in vivo studies presented the direct anti-inflammatory mechanism of silver.

We applied commercially available wound dressings with two different antiseptics. However, the dressings also differed in terms of their construction. While the use of commercially available dressings allowed for a real-world comparison of their performance, it cannot be excluded that some of the impacts on wound healing were due to the differing parameters of the wound dressings (eg, exudate absorption capacity, the presence of hyaluronan). Since the amount of silver varies from one type of silver dressing to another as does the amount of silver that penetrates into the skin,[68] the magnitude of the effects observed in this study may not be the same for other silver dressings. We also acknowledge that our sample size was small in comparison to most other studies that have investigated wound healing under various conditions. We focused to a greater extent on providing a detailed description of the events that occurred during the wound healing process with respect to a smaller group of patients. Nevertheless, our results may serve as the basis for the selection of parameters for investigation using a larger patient cohort.

Silver is used to treat millions of complicated wounds worldwide and it is often perceived as a surface-active antiseptic that is removed with the tissue slough or exudate. We have provided a detailed histological analysis that considers the distribution of silver in chronic wounds and the associated changes in the gene expression in the resident cells. These observations may serve to increase the awareness of clinicians who use silver to treat wounds of the behavior of the metal in wounds. We also demonstrated via a side-by-side comparison approach that a dressing containing octenidine

and hyaluronan supported wound healing more efficiently than did a silver dressing.

ACKNOWLEDGMENTS

We are grateful for the technical assistance provided by Šárka Dušková, Lenka Nespěchalová, and Šárka Průchová. This study was supported by PROGRES Q40/12.

CONFLICT OF INTEREST

VP, MC, KN, and VV are employed by the manufacturer of the OCT-HA dressing (Contipro, Czech Republic). LS, JP, AM, and MA declare no conflicts of interest.

AUTHOR CONTRIBUTIONS

V. Pavlík, L. Sobotka, K. Nešporová, and V. Velebný designed the study. V. Pavlík, L. Sobotka, M. Čepa, J. Pejchal, and A. Mrózková performed the experiments. V. Pavlík, L. Sobotka, M. Čepa, J. Pejchal, A. Mrózková, M. Arenbergerová, and K. Nešporová curated the data. The formal analysis and visualization were performed by V. Pavlík, J. Pejchal, L. Sobotka, M. Čepa, and M. Arenbergerová. The original draft was written by V. Pavlík and J. Pejchal. K. Nešporová, L. Sobotka, M. Čepa, M. Arenbergerová, A. Mrózková, and V. Velebný subsequently reviewed the article. All the authors read and approved the final manuscript.

DATA AVAILABILITY STATEMENT

All the primary data files are available from the figshare database using the digital online identifiers: 10.6084/m9.figshare.11890155, 10.6084/m9.figshare.11855562, 10.6084/m9.figshare.11842413, 10.6084/m9.figshare.11842398, 10.6084/m9.figshare.11842383.

ORCID

Vojtěch Pavlík https://orcid.org/0000-0002-6575-9726
Jaroslav Pejchal https://orcid.org/0000-0003-2228-7922

REFERENCES

1. Olsson M, Järbrink K, Divakar U, et al. The humanistic and economic burden of chronic wounds: a systematic review: the burden of chronic wounds. *Wound Rep Reg*. 2019;27:114-125.
2. Rahim K, Saleha S, Zhu X, Huo L, Basit A, Franco OL. Bacterial contribution in chronicity of wounds. *Microb Ecol*. 2017;73:710-721.
3. Djokić S. Antimicrobial activity of electrochemically oxidized silver and copper. *ECS Trans*. 2010;25:7-15.
4. Djokić SS, Burrell RE. Behavior of silver in physiological solutions. *J Electrochem Soc*. 1998;145:1426-1430.
5. Mijnendonckx K, Leys N, Mahillon J, Silver S, Van Houdt R. Antimicrobial silver: uses, toxicity and potential for resistance. *BioMetals*. 2013;26:609-621.
6. Hwang I, Lee J, Hwang JH, Kim K-J, Lee DG. Silver nanoparticles induce apoptotic cell death in Candida albicans through the increase of hydroxyl radicals. *FEBS J*. 2012;279:1327-1338.
7. Bisson J-F, Hidalgo-Lucas S, Bouschbacher M, Thomassin L. Effects of TLC-Ag dressings on skin inflammation. *J Dermatol*. 2013;40:463-470.
8. Nadworny PL, Landry BK, Wang J, Tredget EE, Burrell RE. Does nanocrystalline silver have a transferable effect? *Wound Repair Regen*. 2010;18:254-265.
9. Vimbela GV, Ngo SM, Fraze C, Yang L, Stout DA. Antibacterial properties and toxicity from metallic nanomaterials. *Int J Nanomedicine*. 2017;12:3941-3965.
10. Zhang X-F, Shen W, Gurunathan S. Silver nanoparticle-mediated cellular responses in various cell lines: an in vitro model. *Int J Mol Sci*. 2016;17:1603.
11. Fumal I, Braham C, Paquet P, Piérard-Franchimont C, Piérard GE. The beneficial toxicity paradox of antimicrobials in leg ulcer healing impaired by a polymicrobial flora: a proof-of-concept study. *Dermatology*. 2002;204(Suppl 1):70-74.
12. Rosen J, Landriscina A, Kutner A, et al. Silver sulfadiazine retards wound healing in mice via alterations in cytokine expression. *J Invest Dermatol*. 2015;135:1459-1462.
13. Barillo DJ, Croutch CR, Barillo AR, Reid F, Singer A. Safety evaluation of silver-ion dressings in a porcine model of deep dermal wounds: a GLP study. *Toxicol Lett*. 2020;319:111-118.
14. Constable JD, Morris PJ, Burke JF, Constable JD. Absorption pattern of silver nitrate from open wounds. *Plast Reconstr Surg*. 1967;39:342-348.
15. Barillo DJ, Croutch CR, Reid F, Culley T, Sosna W, Roseman J. Blood and tissue silver levels following application of silver-based dressings to sulfur mustard chemical burns. *J Burn Care Res*. 2017;38:e818-e823.
16. Pfurtscheller K, Petnehazy T, Goessler W, Bubalo V, Kamolz L-P, Trop M. Transdermal uptake and organ distribution of silver from two different wound dressings in rats after a burn trauma. *Wound Repair Regen*. 2014;22:654-659.
17. Rigo C, Ferroni L, Tocco I, et al. Active silver nanoparticles for wound healing. *Int J Mol Sci*. 2013;14:4817-4840.
18. Coombs CJ, Wan AT, Masterton JP, Conyers RAJ, Pedersen J, Chia YT. Do burn patients have a silver lining? *Burns*. 1992;18:179-184.
19. Hadrup N, Sharma AK, Loeschner K. Toxicity of silver ions, metallic silver, and silver nanoparticle materials after in vivo dermal and mucosal surface exposure: a review. *Regul Toxicol Pharmacol*. 2018;98:257-267.
20. Roman M, Rigo C, Castillo-Michel H, et al. Spatiotemporal distribution and speciation of silver nanoparticles in the healing wound. *Analyst*. 2020;145(20):6456-6469.
21. Hübner N-O, Siebert J, Kramer A. Octenidine dihydrochloride, a modern antiseptic for skin, mucous membranes and wounds. *Skin Pharmacol Physiol*. 2010;23:244-258.
22. Kodedová M, Sigler K, Lemire BD, Gášková D. Fluorescence method for determining the mechanism and speed of action of surface-active drugs on yeast cells. *Biotechniques*. 2011;50:58-63.
23. Malanovic N, Ön A, Pabst G, Zellner A, Lohner K. Octenidine: novel insights into the detailed killing mechanism of Gram-negative bacteria at a cellular and molecular level. *Int J Antimicrob Agents*. 2020;56:106146.
24. Günther F, Blessing B, Dapunt U, Mischnik A, Mutters NT. Ability of chlorhexidine, octenidine, polyhexanide and chloroxylenol to inhibit metabolism of biofilm-forming clinical multidrug-resistant organisms. *J Infect Prev*. 2021;22:12-18.

25. Bührer C, Bahr S, Siebert J, Wettstein R, Geffers C, Obladen M. Use of 2% 2-phenoxyethanol and 0.1% octenidine as antiseptic in premature newborn infants of 23–26 weeks gestation. *J Hosp Infect*. 2002;51:305-307.
26. Vanscheidt W, Harding K, Téot L, Siebert J. Effectiveness and tissue compatibility of a 12-week treatment of chronic venous leg ulcers with an octenidine based antiseptic—a randomized, double-blind controlled study. *Int Wound J*. 2012;9:316-323.
27. Stahl J, Braun M, Siebert J, Kietzmann M. The percutaneous permeation of a combination of 0.1% octenidine dihydrochloride and 2% 2-phenoxyethanol (octenisept®) through skin of different species in vitro. *BMC Vet Res*. 2011;7(1):44.
28. Nikolić N, Kienzl P, Tajpara P, Vierhapper M, Matiasek J, Elbe-Bürger A. The antiseptic octenidine inhibits langerhans cell activation and modulates cytokine expression upon superficial wounding with tape stripping. *J Immunol Res*. 2019;2019:1-11. https://doi.org/10.1155/2019/5143635.
29. Seiser S, Janker L, Zila N, et al. Octenidine-based hydrogel shows anti-inflammatory and protease-inhibitory capacities in wounded human skin. *Sci Rep*. 2021;11:32.
30. Pavlík V, Sojka M, Mazúrová M, Velebný V. Dual role of iodine, silver, chlorhexidine and octenidine as antimicrobial and antiprotease agents. *PLoS ONE*. 2019;14:e0211055.
31. Hämmerle G, Strohal R. Efficacy and cost-effectiveness of octenidine wound gel in the treatment of chronic venous leg ulcers in comparison to modern wound dressings. *Int Wound J*. 2016;13:182-188.
32. Ghatak S, Maytin EV, Mack JA, et al. Roles of proteoglycans and glycosaminoglycans in wound healing and fibrosis. *Int J Cell Biol*. 2015;2015:1-20. https://doi.org/10.1155/2015/834893.
33. Petrey AC, de la Motte CA. Hyaluronan in inflammatory bowel disease: cross-linking inflammation and coagulation. *Matrix Biol*. 2019;78-79:314-323.
34. Cyphert JM, Trempus CS, Garantziotis S. Size matters: molecular weight specificity of hyaluronan effects in cell biology. *Int J Cell Biol*. 2015;2015:563818.
35. Longaker MT, Chiu ES, Adzick NS, Stern M, Harrison MR, Stern R. Studies in fetal wound healing. V. A prolonged presence of hyaluronic acid characterizes fetal wound fluid. *Ann Surg*. 1991;213:292-296.
36. Mahedia M, Shah N, Amirlak B. Clinical evaluation of hyaluronic acid sponge with zinc versus placebo for scar reduction after breast surgery. *Plast Reconstr Surg Glob Open*. 2016;4:e791.
37. Monavarian M, Kader S, Moeinzadeh S, Jabbari E. Regenerative scar-free skin wound healing. *Tissue Eng Part B Rev*. 2019;25:294-311.
38. Catanzano O, D'Esposito V, Acierno S, et al. Alginate-hyaluronan composite hydrogels accelerate wound healing process. *Carbohyd Polym*. 2015;131:407-414.
39. Shatirishvili M, Burk AS, Franz CM, et al. Epidermal-specific deletion of CD44 reveals a function in keratinocytes in response to mechanical stress. *Cell Death Dis*. 2016;7:e2461.
40. Voigt J, Driver VR. Hyaluronic acid and wound healing. *Wound Repair Regen*. 2012;20:317-331.
41. Panuncialman J, Hammerman S, Carson P, Falanga V. Wound edge biopsy sites in chronic wounds heal rapidly and do not result in delayed overall healing of the wound. *Wound Repair Regen*. 2010;18:21-25.
42. Danscher G, Stoltenberg M, Juhl S. How to detect gold, silver and mercury in human brain and other tissues by autometallographic silver amplification. *Neuropathol Appl Neurobiol*. 1994;20:454-467.
43. Sultana J, Molla MR, Kamal M, Shahidullah M, Begum F, Bashar MA. Histological differences in wound healing in Maxillofacial region in patients with or without risk factors. *Bangladesh J Pathol*. 2009;1(24):3-8.
44. Schindelin J, Arganda-Carreras I, Frise E, et al. Fiji: an open-source platform for biological-image analysis. *Nat Methods*. 2012;9:676-682.
45. R Development Core Team. *R: A Language and Environment for Statistical Computing*. Vienna, Austria: R Foundation for Statistical Computing; 2018.
46. Klein P, Sojka M, Kucera J, et al. A porcine model of skin wound infected with a polybacterial biofilm. *Biofouling*. 2018;34:226-236.
47. Livak KJ, Schmittgen TD. Analysis of relative gene expression data using real-time quantitative PCR and the $2-\Delta\Delta CT$ method. *Methods*. 2001;25:402-408.
48. Tak YK, Pal S, Naoghare PK, Rangasamy S, Song JM. Shape-dependent skin penetration of silver nanoparticles: does it really matter? *Sci Rep*. 2015;5:16908.
49. Fredriksson C, Kratz G, Huss F. Accumulation of silver and delayed re-epithelialization in normal human skin: an ex-vivo study of different silver dressings. *Wounds*. 2009;21:116-123.
50. Trop M, Novak M, Rodl S, Hellbom B, Kroell W, Goessler W. Silver-coated dressing acticoat caused raised liver enzymes and argyria-like symptoms in burn patient. *J Trauma*. 2006;60:648-652.
51. Mulley G, Jenkins ATA, Waterfield NR. Inactivation of the antibacterial and cytotoxic properties of silver ions by biologically relevant compounds. *PLoS ONE*. 2014;9:e94409.
52. Brouillard C, Bursztejn AC, Latarche C, et al. Silver absorption and toxicity evaluation of silver wound dressings in 40 patients with chronic wounds. *J Eur Acad Dermatol Venereol*. 2018;32(12):2295-2299.
53. Dalzon B, Aude-Garcia C, Diemer H, et al. The longer the worse: a combined proteomic and targeted study of the long-term versus short-term effects of silver nanoparticles on macrophages. *Environ Sci Nano*. 2020;7:2032-2046.
54. Brzicova T, Javorkova E, Vrbova K, et al. Molecular responses in THP-1 macrophage-like cells exposed to diverse nanoparticles. *Nanomaterials*. 2019;9:687.
55. Paul A, Ju H, Rangasamy S, Shim Y, Song JM. Nanosized silver (II) pyridoxine complex to cause greater inflammatory response and less cytotoxicity to RAW264.7 macrophage cells. *Nanoscale Res Lett*. 2015;10:140.
56. Souza HR, de Azevedo LR, Possebon L, et al. Heterogeneity of mast cells and expression of Annexin A1 protein in a second degree burn model with silver sulfadiazine treatment. *PLoS ONE*. 2017;12:e0173417.
57. Shim I, Choi K, Hirano S. Oxidative stress and cytotoxic effects of silver ion in mouse lung macrophages J774.1 cells. *J Appl Toxicol*. 2017;37:471-478.
58. Kaewamatawong T, Banlunara W, Maneewattanapinyo P, Thammachareon C, Ekgasit S. Acute and subacute pulmonary toxicity caused by a single intratracheal instillation of colloidal silver nanoparticles in mice: pathobiological changes and metallothionein responses. *J Environ Pathol Toxicol Oncol*. 2014;33:59-68.
59. Lansdown AB, Sampson B, Laupattarakasem P, Vuttivirojana A. Silver aids healing in the sterile skin wound: experimental studies in the laboratory rat. *Br J Dermatol*. 1997;137:728-735.
60. Inoue K, Takano H, Shimada A, Satoh M. Metallothionein as an anti-inflammatory mediator. *Mediators Inflamm*. 2009;2009:1-7.
61. Krasowski G, Jawień A, Tukiendorf A, et al. A comparison of an antibacterial sandwich dressing vs dressing containing silver. *Wound Repair Regen*. 2015;23:525-530.

62. Winter H, Haas N. Granulation tissue flap technique in extensive wounds for covering exposed bone after tumor excision. *Dermatol Surg*. 2000;26:829-834.
63. Chen Z, Dai T, Chen X, Tan L, Shi C. Activation and regulation of the granulation tissue derived cells with stemness-related properties. *Stem Cell Res Ther*. 2015;6:85.
64. Hartmann CA, Rode H, Kramer B. Acticoat™ stimulates inflammation, but does not delay healing, in acute full-thickness excisional wounds. *Int Wound J*. 2016;13:1344-1348.
65. Nadworny PL, Wang J, Tredget EE, Burrell RE. Anti-inflammatory activity of nanocrystalline silver-derived solutions in porcine contact dermatitis. *J Inflamm*. 2010;7:13.
66. Thomason HA, Lovett JM, Spina CJ, Stephenson C, McBain AJ, Hardman MJ. Silver oxysalts promote cutaneous wound healing independent of infection. *Wound Repair Regen*. 2018;26(2):144-152.
67. You C, Li Q, Wang X, et al. Silver nanoparticle loaded collagen/chitosan scaffolds promote wound healing via regulating fibroblast migration and macrophage activation. *Sci Rep*. 2017;7:10489.
68. Nešporová K, Pavlík V, Šafránková B, et al. Effects of wound dressings containing silver on skin and immune cells. *Sci Rep*. 2020;10:15216.

SUPPORTING INFORMATION

Additional Supporting Information may be found online in the Supporting Information section.

How to cite this article: Pavlík V, Sobotka L, Pejchal J, et al. Silver distribution in chronic wounds and the healing dynamics of chronic wounds treated with dressings containing silver and octenidine. *The FASEB Journal*. 2021;35:e21580. https://doi.org/10.1096/fj.202100065R